ORIGINAL ARTICLE

Establishing cell suitability for high-level production of licorice triterpenoids in yeast

Wentao Sun [a,d,e], **Shengtong Wan** [b], **Chuyan Liu** [c], **Ruwen Wang** [b], **Haocheng Zhang** [a,d,e], **Lei Qin** [a,d,e], **Runming Wang** [f], **Bo Lv** [b,*], **Chun Li** [a,b,d,e,*]

[a]*Department of Chemical Engineering, Tsinghua University, Beijing 100084, China*
[b]*Key Laboratory of Medical Molecule Science and Pharmaceutics Engineering, Ministry of Industry and Information Technology, Institute of Biochemical Engineering, School of Chemistry and Chemical Engineering, Beijing Institute of Technology, Beijing 100081, China*
[c]*The University of Chicago, Chicago, IL 60637, USA*
[d]*Key Lab for Industrial Biocatalysis, Ministry of Education, Tsinghua University, Beijing 100084, China*
[e]*Center for Synthetic and Systems Biology, Tsinghua University, Beijing 100084, China*
[f]*Institute of Biopharmaceutical and Health Engineering, Tsinghua Shenzhen International Graduate School, Tsinghua University, Shenzhen 518055, China*

Abstract Yeast has been an indispensable host for synthesizing complex plant-derived natural compounds, yet the yields remained largely constrained. This limitation mainly arises from overlooking the importance of cell and pathway suitability during the optimization of enzymes and pathways. Herein, beyond conventional enzyme engineering, we dissected metabolic suitability with a framework for simultaneously augmenting cofactors and carbon flux to enhance the biosynthesis of heterogenous triterpenoids. We further developed phospholipid microenvironment engineering strategies, dramatically improving yeast's suitability for the high performance of endoplasmic reticulum (ER)-localized, rate-limiting plant P450s. Combining metabolic and microenvironment suitability by manipulating only three genes, *NHMGR* (NADH-dependent HMG-CoA reductase), *SIP4* (a DNA-binding transcription factor)and *GPP1* (Glycerol-1-phosphate phosphohydrolase 1), we enabled the high-level production of 4.92 g/L rare licorice triterpenoids derived from consecutive oxidation of β-amyrin by two P450 enzymes after fermentation optimization. This production holds substantial commercial value, highlighting the critical role of establishing cell suitability in enhancing triterpenoid biosynthesis and offering a versatile framework applicable to various plant natural product biosynthetic pathways.

1. Introduction

Over the past decade, the *de novo* biosynthesis of natural pharmaceutical compounds in microbes has been achieved through the introduction of heterologous genes[1,2]. *Saccharomyces cerevisiae* has emerged as a main host for this purpose due to its safety, genetic manipulability, and intrinsic endomembrane system, particularly suited for the production of complex natural products reliant on membrane-localized cytochrome P450 enzymes (P450), such as plant triterpenoids, cannabinoids, and alkaloids[3-6]. Despite these advancements, the titers of natural pharmaceutical compounds remain to be significantly improved, notably due to the limited efficiency of heterogeneous biosynthesis pathways in yeast[7], exemplified by licorice triterpenoids[8].

Licorice triterpenoids, comprising diverse oleanolic-type triterpenoids with notable physiological benefits, are derived from the roots of the renowned licorice plant, long esteemed in traditional medicinal practices. Among these compounds, 11-oxo-β-amyrin, glycyrrhetaldehyde, and glycyrrhetinic acid stand out as a rare subset of licorice triterpenoids with low abundance in licorice roots but exhibit a wide spectrum of physiological and pharmaceutical activities[9-15]. Although heterologous biosynthesis within *Saccharomyces cerevisiae* has been demonstrated as a feasible approach, its industrial application remains challenging due to the inefficiencies of the biosynthetic pathway[8,16].

Pathway engineering has been extensively employed to bolster production; however, current research predominantly focuses on pathway refinement, often overlooking the critical role of cell and pathway compatibility in enhancing microbial production of natural products. Despite the implementation of various strategies aimed at amplifying precursor supply, downregulating *ERG7* expression, and reinforcing NADPH regeneration to elevate triterpenoid biosynthesis, limited efficacy persists in the biosynthesis of many plant triterpenoids, including 11-oxo-β-amyrin[12], glycyrrhetinic acid[8] and oleanolic acid[17], etc. Moreover, approaches aimed at promoting precursor synthesis by enhancing MEP and MVA pathways and overexpressing numerous related genes may impose metabolic burden and threaten genomic stability in engineered strains[2,4,18,19]. Notably, strategies aimed at creating a suitable metabolic framework for heterologous biosynthesis in pathway refinement remain sparse. Unraveling the metabolic suitability for natural product biosynthesis in yeast holds significant promise to expand the scope of metabolic engineering endeavors, facilitating the efficient production of phytochemicals with minimal genetic manipulation.

Together with the unelucidated metabolic suitability, the limited performance of key enzymes also considerably restricts biosynthetic efficiency. The notably limited functionality of P450 enzymes within microbial cell factories is widely acknowledged as the principal rate-limiting factor in the biosynthesis of many plant natural products. For instance, the low activity of G8H (geraniol 8-hydroxylase) leads to the production of strictosidine at exceedingly low titers in yeast[20]. The biosynthesis of rare licorice triterpenoids faces a similar bottleneck due to low P450 enzyme performance. This process begins with the conversion of β-amyrin into 11-oxo-β-amyrin through the oxidation of C-11 by Uni25647. Next, CYP72A63 oxidizes the C-30 of 11-oxo-β-amyrin to form glycyrrhetaldehyde and glycyrrhetinic acid, consecutively[8,16,21].

In previous studies, efforts were made to mitigate this limitation by redesigning CYP72A63 and creating a high-activity mutant, CYP72A63 (T338S), to enhance glycyrrhetinic acid production. Despite these interventions, the achieved titer remained confined to 36 mg/L[21]. While protein engineering holds promise in enhancing the activity of plant enzymes in yeast, the enzyme microenvironment exerts significant influence on catalytic activities[22,23]. As endoplasmic reticulum (ER)-located NADPH-dependent enzymes, P450 performance is largely affected by intracellular NADPH availability and the surrounding phospholipid microenvironment. Nevertheless, the importance and necessity of engineering the host's internal microenvironment, especially the phospholipid microenvironment, to facilitate high performance of heterologous P450 enzymes, are often overlooked in engineering endeavors.

To address these challenges and enhance phytochemical production, we devised systematic strategies integrating conventional protein engineering and elucidated cell suitability, simultaneously enhancing precursor supply, cofactor availability to heterologous pathways, and microenvironment suitability for heterologous enzymes with minimal strain burden. This comprehensive approach resulted in increased enzymatic activity, robust cofactor supply, enhanced carbon flux provision, and tailored phospholipid microenvironment, thereby facilitating exceptional performance of plant P450 enzymes and significantly intensifying the efficiency of heterologous biosynthesis pathways (Fig. 1). Notably, these achievements were accomplished through the manipulation of only three genes, *NHMGR*, *SIP4*, and *GPP1*. When combined with fermentation engineering, this approach yielded high-level licorice triterpenoid production with promising commercial applicability. Our findings present innovative avenues for enhancing heterologous biosynthetic pathways and offer novel strategies for efficiently producing natural products in yeast.

2. Materials and methods

2.1. Molecular docking and substrate tunnel analysis

The 3D structures of Uni25647 were constructed by Alphafold 2. ADFRsuite-1.0 and Autodock vina were used for molecular docking. A grid box of 20 × 20 × 20, which encompassed the active pocket of Uni25647, was set as the search space to explore suitable compound I binding modes[41]. The PDBQT format was employed for both the input and output of molecular structures. The models with docked compound I in appropriate position were used for analysis. The substrate tunnel was then analyzed with Caver_analyst2 using the oxygen atom of the compound I as the starting point.
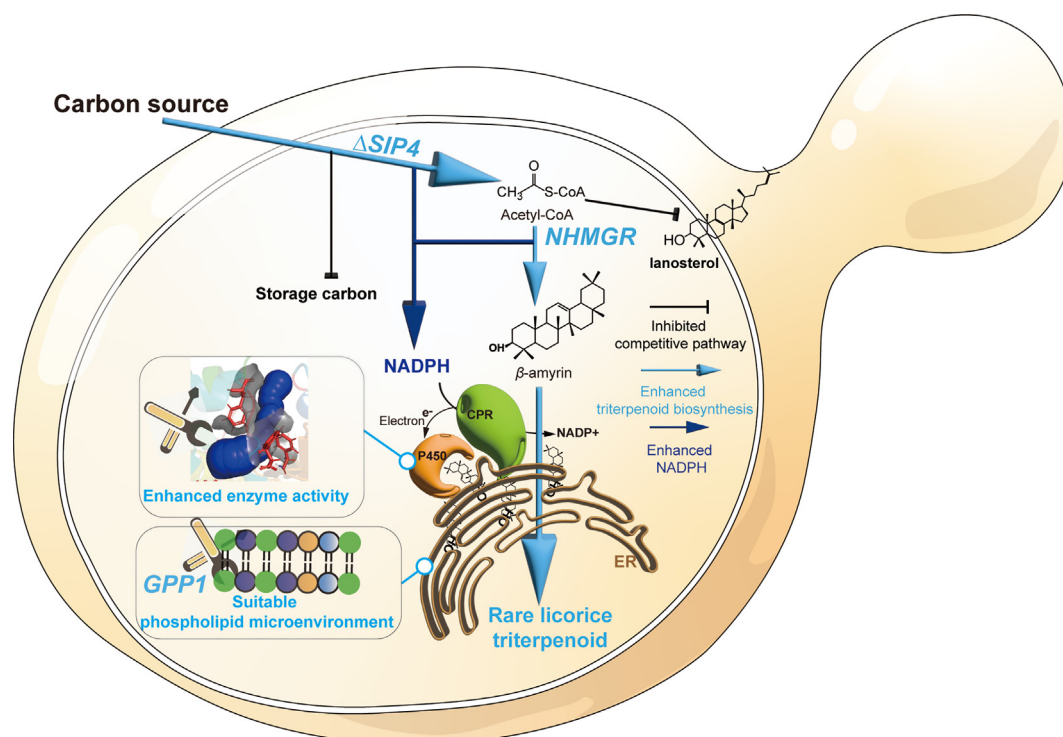
Figure 1 Creating metabolic and microenvironment suitability to facilitate the exceptional performance of plant triterpenoids biosynthesis in yeast. Blue and baby blue arrows indicate intensified pathways while black blunt arrows indicate inhibited pathways.

2.2. Construction of gene expression cassettes

The sequences used for the construction of the expression cassette are listed behind. Gibson assembly was used for the plasmid construction. Fragments of promoter, terminator and the sequence of the homologous domain were amplified from the genomic DNA of *Saccharomyces cerevisiae* SynV. PrimeSTAR HS DNA polymerase (TaKaRa, China) was used for DNA cloning. The resulting DNA fragments and plasmids were purified using a TIANgel Midi Purification Kit and a TIANprep Midi Plasmid Kit (TIANGEN BIOTECH, China). Original candidate genes were amplified with PCR. The constructed DNA fragments were ligated into a pMD19-T vector and were subsequently sequenced for confirmation.

2.3. Site-specific mutagenesis

The site-specific mutagenesis library was constructed by the Fast Mutagenesis System (FM111, TransGen Biotech, China). The primers were listed in Supporting Information Table S1.

2.4. Construction of yeast strains

The *S. cerevisiae* SynV[24] was used as the host strain in this study. The LiAc/SS carrier DNA-PEG method was used for the yeast transformation[25]. The synthetic pathway for the licorice triterpenoids was constructed using the DNA assembler strategy as described by the Zhao group[26]. Briefly, the coding sequences for β-amyrin synthase (GgbAS), Uni25647, CYP72A63(T338S) were codon-optimized according to yeast codon preference. For each cassette, the ORF, its corresponding promoter and terminator, together with the homologous domain were connected by adjacent parts. For genome integration, the *HIS3*, *Leu2*, *URA3* auxotrophic

markers, G418 and *ble* (Bleomycin resistance gene) markers were used. The strains used in this study are listed in Supporting Information Table S2. All the strains used for the verification of the mutants were derived from SynV carrying the synthesized chromosome V. The Uni25647 mutant was introduced into the SynV8 (Table S2) together with *GgbAS*, *GuCPR1*(P450 reductase), and *ERG1*. The genotype of the constructed strain was as followed: SynV8:*ΔHO::FBA1p-bAS-CYC1t-Gal7p-Uni25647mutants-TYS1t-PGK1p-GuCPR1-PGK1t-HSP12p-ERG1-PYK1t-G418*.

2.5. Medium and growth conditions for yeast harboring licorice biosynthetic pathway

YPD medium containing 10 g/L yeast extract, 20 g/L peptone and 20 g/L glucose and the optimized medium containing 10 g/L yeast extraction, 20 g/L glucose and 10 g/L corn steep liquor were used in this work. The engineered yeast strains were pre-cultured in 2 ml YPD medium at 30 °C, 200 rpm for 24 h. Then, the strains were inoculated into 50 mL fresh YPD or optimized medium in flasks. Subsequently, the strains were cultivated for 120 h for the accumulation of target compounds.

2.6. In vitro enzymatic activity assay

In vitro enzymatic activity assay of P450s was conducted using microsome, which were prepare as previously described[27]. Microsomal membranes were suspended in storage buffer containing 50 mmol/L Tris-HCl (pH 7.5), 1 mmol/L EDTA, and 20% (v/v) glycerol. Initial *in vitro* oxidation assays were conducted in a total volume of 500 μL, containing 1 mmol/L NADPH, 1 mg of microsomal protein, and 100 μmol/L β-amyrin. The assays were incubated with shaking for 24 h at 30 °C, and the reactions were

terminated by extraction with 1 mL of ethyl acetate. These extracts were then analyzed with GC−MS.

2.7. Fed-batch fermentation

For larger-scale cultures, a 5 L fermentor (Parallel-Bioreactor Co., Ltd., China) containing 2.5 L of fermentation medium was adopted. The recombinant yeast strain precultured in YPD or the optimized medium in shake flask was used as the inoculum and the inoculation volume was 10%. The composition of the fermentation medium was YPD or the optimized medium containing 10 g/L yeast extraction, 20 g/L glucose and 10 g/L corn steep liquor. To obtain a high cell density, the strains were auxotrophically recovered before used in larger-scale cultures. Fermentations were carried out at 30 °C, and pH was controlled at 5.0 by the automatic addition of 5 mol/L ammonia hydroxide. Dissolved oxygen (DO) was maintained at 25%−40% saturation by adjusting the agitation rate (300−800 rpm) and airflow rate (1−3 vvm).

2.8. Compound extraction and analysis

After cultivation, 1 mL of yeast cell culture was treated by a sample grinder, and then were extracted using ethyl acetate. The resulting extracts and aqueous-phase were respectively pooled, dried, and trimethylsilylated with pyridine and N,O-bis (trimethylsilyl) trifluoroacetamide (BSTFA) for analysis of licorice triterpenoids and the metabolites derived from central carbon metabolism and gluconeogenesis such as succinate, malate, fumarate and trehalose by GC−MS.

The GC−MS analysis was performed using an Agilent 8890-5977B GC/MSD Ultra (Agilent Technologies) equipped with an Agilent 19091S-433. J&W HP-5ms GC Column (30 m × 0.25 mm × 0.25 μm, Agilent, USA) GC column with a carrier gas helium flow of 1.5 mL/min, using a split mode; split ratio was 5:1. For the detection of licorice triterpenoids, the compound separation procedure was as follows: injector temperature 250 °C; column temperature start with 80 °C for 1 min, 290 °C for 38 min at a 20 °C/min increase; ion source temperature 200 °C and interface temperature set to 290 °C, using scan mode and monitoring the m/z range from 50 to 700 with a solvent delay of 18 min. For the detection GC−MS based metabolomics, the compound separation procedure was as follows: injector temperature 250 °C; column temperature start with 60 °C for 1 min, 310 °C for 14 min at a 10 °C/min increase; ion source temperature 200 °C and interface temperature set to 290 °C, using scan mode and monitoring the m/z range from 50 to 800 with a solvent delay of 3.8 min. Squalene, organic acids, ergosterol, lanosterol, β-amyrin, glycyrrhetinic acid standard (purchased from Sigma−Aldrich), 11-oxo-β-amyrin (purchased from BioBioPha, China) standard were used for quantification. Glycyrrhetaldehyde purified from the products by yeast strain GA184. For its extraction, the culture was smashed by High Pressure Homogenizer (1500 MPa). Ethyl acetate was used to extract the triterpenoids from the smash, and the supernatant was collected and dried by rotary evaporators. Methanol was used to dissolve the dried material. The solution was used for separation of glycyrrhetaldehyde on semi-preparing liquid chromatography (DGU-12AM, Shimadzu Scientific Instruments) equipped with a PRC-ODS (H) column (Shimadzu Scientific Instruments) after filtration by 0.22 μm filter membrane. Mobile phase A was 0.6% acetic acid solution, mobile phase B was methanol, A:B = 1:4, flow rate = 5 mL/min, detection wavelength was 254 nm. Calculation of the concentration was based on external standard method. In this study, total licorice triterpenoids included, 11-oxo-β-amyrin, glycyrrhetaldehyde and glycyrrhetinic acid.

The concentration of glucose, succinate, ethanol, glycerol and trehalose was detected by HPLC analysis which was performed using an Agilent 1260 Infinity II equipped with a Aminex HPX-87H (300 mm × 7.8 mm) column and a RID detection. Mobile phase 5 mmol/L H_2SO_4, flow speed 0.6 mL/min, RID temperature 50 °C, column temperature 55 °C. The standard curves were listed in Supporting Information Fig. S1.

2.9. Transcriptome profiling

Strains were incubated in YPD media at 30 °C, 200 rpm for proper time. Samples for RNA-seq were taken and stored at −80 °C. Samples were determined in duplicates from the individual incubations. The RNA-seq test was conducted using the Illumina TruSeq platform. RSEM was used to calculate FPKM values. Analysis of differential expression was performed using PossionDis. Differentially expressed genes were defined as genes with a Ilog2foldchangeI ≥1.0, and significantly different genes were defined as genes with a Ilog2foldchangeI ≥1.5. The RNA-seq data were deposited to NCBI with an accession number PRJNA967798.

2.10. Assays of NADPH, NADH and ATP

NADPH content was determined using the Coenzyme II NADP(H) Content Assay Kit (Solarbio, China). NADH content was determined using NAD^+/NADH Assay Kit with WST-8 (Beyotime, China). ATP content was determined using the ATP Content Assay Kit (Solarbio, China).

2.11. Real-time reverse transcription-PCR

The total RNA was extracted from yeast cells by Trizol and served as the template to obtain complementary DNA using the TransScript First-Strand cDNA Synthesis Kit (Trans, China). The converted cDNA and the specific primers were added to Top/Tip Green qRCR SuperMix to subject RT-PCR analysis employing the Roche LightCycler 96 Real-Time PCR System (Cal, USA). ACT1 was selected as the internal reference gene. Primes used for qPCR were listed in Supporting Information Table S3.

2.12. Lipidomics analysis

To analyze the changes in phospholipid of membrane, lipidomics analysis was conducted for GA184, and strains overxpressing GPP1. Cells cultivated in YPD for 48h were collected for lipid detection. The ER was firstly extracted using an ER extraction kit (beibokit, China), which was subsequently used for lipid extraction. Total ER lipids were extracted according to methods described previously[28] and detected by the UPLC system was coupled to a Q-Exactive HFX orbitrap mass spectrometer (Thermo Fisher, CA, USA) equipped with a heated electrospray ionization (HESI) probe. Lipid extracts were separated by a Cortecs C18 100 mm × 2.1 mm column (Waters). A binary solvent system was used, in which mobile phase A consisted of ACN: H2O (60:40), 10 mmol/L ammonium acetate, and mobile phase B of IPA: ACN (90:10), 10 mmol/L ammonium acetate. A 35-min gradient with flow rate of 250 μL/min was used. Column chamber and sample tray were held at 40 and 10 °C, respectively. Data
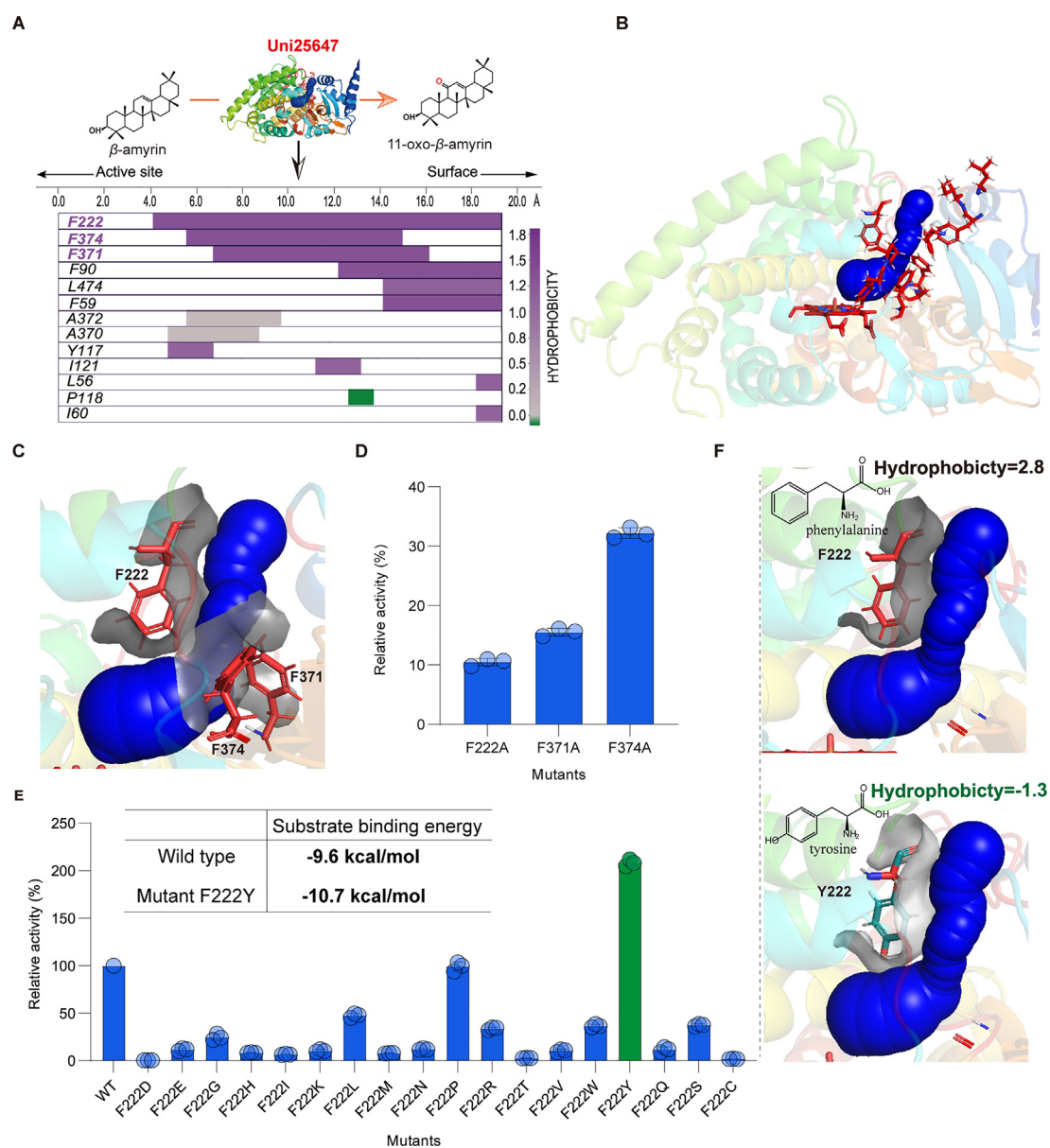
Figure 2 Pathway enhancement by P450 engineering in yeast. (A, B) 3D structure of Uni25647 (the first rate-limiting P450 in licorice triterpenoid biosynthesis) was predicted using Alphafold2, and the substrate tunnel was analyzed using CAVER_Analyst 2; the color bar length indicates the scope of influence on the tunnel of each residue. (C) F374, F371 and F222 formed the bottleneck of the tunnel and F222 had maximum range of influence on the tunnel. (D) The alanine scanning of the bottleneck residues F374, F371 and F222 revealed that perturbation on F222 had the most significant impact on enzyme activity. (E) The Relative activity of Uni25647 mutants at F222 site compared with the wild type (WT, 100% activity) and the substrate binding energy (calculated by AutoDock Vina) of wild type and mutant F222Y. (F) Y222 mutant significantly downregulated the hydrophobicity in the tunnel. Data are presented as mean ± SD ($n = 3$ biologically independent samples).

with mass ranges of m/z 240−2000 and m/z 200−2000 was acquired at positive ion mode and negative ion mode with data dependent MSMS acquisition. The full scan and fragment spectra were collected with resolution of 60,000 and 15,000, respectively. The source parameters are as follows: spray voltage: 3000 v; capillary temperature: 320 °C; heater temperature: 300 °C; sheath gas flow rate: 35 Arb; auxiliary gas flow rate: 10 Arb. Data analysis and lipid identification were performed by the software lipidsearch (Thermo Fisher, CA, USA). All of molecular identifications were based on MS2, with a MS1 mass error of <5 ppm and MS2 mass error of <8 ppm. Relative lipid content was used in

this study, which was calculated by the ratio of peak area between g DCW.

3. Results

3.1. Bioreaction enhancement by P450 engineering in yeast

In microbial cell factory, carbon partition is frequently hindered by the low-flux biosynthetic pathways, which result from metabolic rigidity of host cells[29]. Specifically, the restricted

biosynthetic flow is attributed to the limited performance of key enzymes, such as the P450 enzymes involved in rare licorice triterpenoids biosynthesis. Uni25647 is the first committed P450 in biosynthesis of 11-oxo-β-amyrin, glycyrrhetaldehyde, and glycyrrhetinic acid (Fig. 2A, Supporting Information Fig. S2A). To increase the metabolic flux toward the desired pathways, we engineered this rate limiting enzyme for higher catalytic activity. Previously we found the substrate tunnel's high hydrophobicity limits the binding of compound with hydrophilic groups[21]. To investigate the potential influence of substrate tunnel microenvironment on substrate binding and catalytic activity, we generated the 3D model of Uni25647 using AlphaFold2[30]. Substrate tunnel analysis identified the exposed residues to be F222, F371, F374, F90, F59, L474, A372, A370, Y117, I121, P118, L56, and I60 (Fig. 2A and B). Among these, the five hydrophobic amino acid residues, F222, F371, F374, F90, and F59, formed the main body of the tunnel, while F371, F374, and F222 formed a bottleneck and contributed most to the tunnel's hydrophobicity (Fig. 2A and C). Among them, F222 produced a hydrophobic effect within the tunnel from entrance tail to the active pocket (Fig. 2A and C). The hydrophobic nature of the tunnel may repel the hydrophilic hydroxy group at the C-3 tail of β-amyrin. Therefore, we hypothesize slight downregulation of the hydrophobicity in tunnel promotes the enzyme activity.

The alanine scanning of F371, F374, F222 showed that perturbation on F222 generated the greatest impact on Uni25647 activity (Fig. 2C and D), further suggesting the key role of this site on substrate recognition and binding. Therefore, site-directed saturation mutagenesis was conducted on F222. Catalytic activity of all mutants was assessed through 11-oxo-β-amyrin production in *Saccharomyces cerevisiae* SynV carrying β-amyrin and P450 reductase (Table S2). Notably, mutant F222Y was identified with 2.08-fold increased catalytic activity in yeast with a 11-oxo-β-amyrin production of 154.64 $\pm$ 4.76 mg/L and no significant change on protein expression levels (Fig. 2E, Figs. S2B and S2C). Introducing a hydrophilic hydroxy group in F222Y mutant results in reduced hydrophobicity in the substrate tunnel (Fig. 2F). Substrate binding energy was decreased from -9.6 kcal/mol (wild type) to -10.7 kcal/mol (mutant F222Y), indicating refined substrate binding affinities (Fig. 2E). As a result, the catalytic activity of Uni25647 was doubled in F222Y mutant, enhancing the metabolic flux to licorice triterpenoid biosynthesis. Upon introducing *tHMG1*, the commonly used strategy to enhance precursor supply in triterpenoid biosynthesis, the resultant strain GA11-O could produce 178.54 $\pm$ 8.86 mg/L 11-oxo-β-amyrin in flask and 1598.53 $\pm$ 98.81 mg/L 11-oxo-β-amyrin in a 5L fermenter, representing the highest level at present (Fig. S2B and S2D).

3.2. Decoding the metabolic framework suitable for triterpenoid biosynthesis

Based on the enhanced 11-oxo-β-amyrin production, the high-efficiency 11-oxo-β-amyrin oxidase CYP72A63(T338S) was introduced into the *HO* loci of strain GA11-O to produce glycyrrhetaldehyde and glycyrrhetinic acid, resulting in the strain GA182 (Table S2, Fig. S2A). However, the strain GA182 produced only 79.13 $\pm$ 2.55 mg/L rare licorice triterpenoids, less than GA11-O (178.54 $\pm$ 8.86 mg/L), including 48.12 $\pm$ 1.47 mg/L glycyrrhetinic acid and 5.81 $\pm$ 0.61 mg/L glycyrrhetaldehyde (Supporting Information Fig. S3A). Evidently, strain GA183, in the absence of tHMG1, exhibited elevated NADPH levels and

better growth performance when compared to strain GA182 (Fig. 3A, Fig. S3B). This suggests that the current engineering endeavors focusing on reinforcing the associated biosynthetic pathway without due consideration of the suitable metabolic framework would lead to poor suitability to the licorice triterpenoid biosynthesis.

Of note, we found an enhanced rate of total licorice triterpenoid accumulation at 48 h as compared to the 24 h point in GA183, suggesting a reconfigured cellular metabolic framework better suited for triterpenoid biosynthesis at 48 h (Fig. 3B). Transcription analysis revealed down-regulation in the Embden-Meyerhof-Parnas (EMP) pathway, the Pentose Phosphate Pathway (PPP), and even the endogenous MVA pathways, while the licorice triterpenoid pathway remained unaltered (Fig. 3C), suggesting that the pivotal factors underpinning efficient triterpenoid biosynthesis extend beyond these commonly considered pathways.

Notably, the predominant carbon source employed in triterpenoid production was ethanol, as glucose was entirely converted into ethanol before 24 h (Fig. 3B). Consequently, the glyoxylate cycle and gluconeogenesis-linked pathways play pivotal roles in both facilitating strain growth and replenishing crucial cofactors. The related transcriptional analysis revealed three pivotal enzymes—two involved in the glyoxylate cycle, *MLS1* (malate synthase) and *ICL1* (isocitrate lyase), and *PCK1* (phosphoenolpyruvate carboxykinase) governing gluconeogenesis—that serve as central connectors, bridging a metabolic framework fine-tuned for efficient triterpenoid biosynthesis. This role is further validated as the deletion of these enzymes results in a sharp reduction in both licorice triterpenoid production and cell growth (Fig. 3D and E, Fig. S3B). In this metabolic framework, significantly upregulated IDP2 and ALD6 contribute to the supply of essential NADPH, and the production of 2-oxoglutarate and succinate can be translocated to the mitochondria by SFC1 and YHM2 to support the energy requirements essential for cell growth. Concurrently, the up-regulation of PCK1, PDC6, ALD6, and ACS1 facilitates the redirection of metabolic flux towards triterpenoid precursor acetyl-CoA (Fig. 3E).

As a result, directing the acetyl-CoA into triterpenoid efficiently while boosting the NADPH availability, especially in rapid synthesis phase of triterpenoid, would build the metabolic suitability for triterpenoid biosynthesis. To achieve this goal in the most concise and effective manner possible, we used *NHMGR*, a NADH-dependent HMG-CoA reductase (NADH-HMGR) from *Silicibacter pomeroyi*[31,32] instead of *tHMG1* to strengthen the MVA pathway and liberate more NADPH (Fig. 3E). Of note, the resultant strain GA184 exhibited a dramatically promoted performance. The glycyrrhetinic acid and glycyrrhetaldehyde production increased up to 111.40 $\pm$ 10.35 and 66.61 $\pm$ 2.14 mg/L respectively, and the total licorice triterpenoids production increased by 3.84-fold—303.49 $\pm$ 16.67 mg/L (Fig. 3F, Fig. S3A and S3C), while the conversion rate of glucose to licorice triterpenoids increased from 0.40% to 1.52%. The production of precursor β-amyrin increased by 2.80-fold (Fig. 3G) accompanied with improved cell growth by 21.42%. The intracellular NADPH/NADP$^+$ ratio was significantly rescued in GA184, unlocking the NADPH limitation for performance of P450s and enhanced metabolic flux to the target compound (Fig. 3H). Compared with GA182, 0.50 mmol/L more licorice triterpenoids were produced, indicating at least an additional 0.50 mmol/L NADPH was directed to Uni25647(F222Y) and CYP72A63(T338S). Importantly, not only did the NADPH level increase, but its level at 48 h
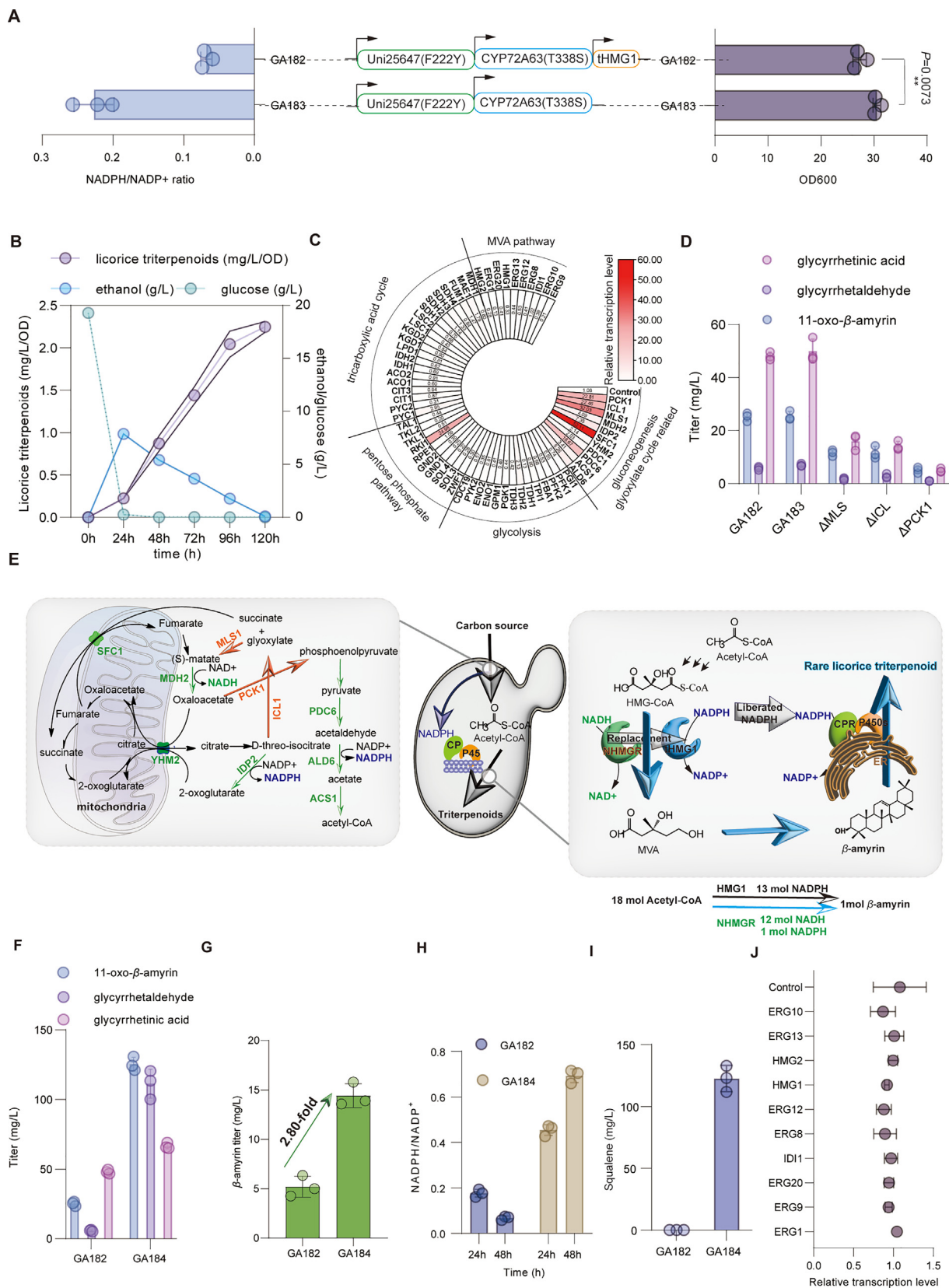
Figure 3 Decoding the metabolic framework suitable for triterpenoid biosynthesis. (A) The NADPH level and growth performance of engineered strains harboring *tHMG1*. (B) Fermentation performance of GA183 in flask. (C) The relative transcriptional level of gluconeogenesis, glycolysis, pentose phosphate pathway, tricarboxylic acid cycle, glyoxylate cycle and MVA pathway in GA183. (D) Perturbation of glyoxylate cycle and gluconeogenesis decreased triterpenoids production. (E) The metabolic framework adapted to

also elevated, when the triterpenoids were rapidly synthesized and significantly exceeding those at 24 h in GA184; this contrasts with GA182, where NADPH levels were notably lower at 48 h compared to 24 h (Fig. 3H). However, due to the high availability and recovery capability of NADH in *Saccharomyces cerevisiae*[33], overexpressing *NHMGR* had no significant reduction on the NADH/NAD$^+$ ratio in GA184 compare to that in GA182 (Fig. S3D). These findings indicated enhanced metabolic suitability of yeast for heterogenous triterpenoids pathway. Moreover, the production of the common triterpenoid precursor squalene was also significantly enhanced (Fig. 3I) while the expression level of related genes in MVA pathway showed no significant difference (Fig. 3J) between GA184 and GA183, suggesting the increased triterpenoids production was mainly due to the metabolic suitability created by the overexpression of *NHMGR*. These results highlighted the importance of creating host-pathway suitability in enhancing heterogenous biosynthesis pathway in yeast. Through this scheme, a more suitable metabolic framework was established with simultaneously enhanced precursor supply, cofactor availability and P450 performance for intensified production and substrate conversion efficiency by overexpressing a single gene.

3.3. Redesigning yeast metabolism to enhance the metabolic suitability

To further refine the metabolic framework, we pursued a concurrent overexpression approach involving *MLS1*, *ICL1* and *PCK1* in GA184, resulting in the strain GA185. However, this strategy of over-enhancement decreased the licorice triterpenoid production (Fig. 4A). Production of succinate, fumarate and malate largely increased, forming a metabolic imbalance that favored primary metabolism over triterpenoid biosynthesis (Supporting Information Fig. S4A).

To circumvent this issue and tenderly regulate these pathways to redirect more metabolic flux to triterpenoids biosynthesis, related transcription factors were screened using SGD database[34-36]. We identified transcription factor *SIP4*[37], known to regulate *ICL1* and gluconeogenesis, and *TOG1*[35] which regulates *MLS1*, *ICL1* and *PCK1*. *SIP4* and *TOG1* were thereby overexpressed and deleted in GA184 to mildly regulate these pathways. Contrary to our expectations, deleting *SIP4* not only significantly promoted licorice triterpenoids production (Fig. 4A and B), but also slightly promoted the endogenous lanosterol production (Fig. S4B), indicating enlarged metabolic flux to triterpenoid biosynthesis and enhanced suitability for triterpenoids biosynthesis. To track the cellular metabolic rearrangement, transcriptome analysis was conducted for GA184 and GA184-ΔSIP4 at 48 h when the licorice triterpenoid was rapidly produced. A moderate metabolism change was found with only 123 differentially expressed genes (Fig. S4C). Interestingly, deleting *SIP4* did not show global changes in gluconeogenesis regulation. Among the key genes involved in the glyoxylate cycle and gluconeogenesis (*ICL1*, *MLS1* and *PCK1*), only *PCK1* showed an up-regulation (Fig. 4B, Fig. S4C). Indeed, overexpressing *PCK1* increased the licorice

triterpenoid production (Fig. 4C), but the enhancement achieved through *PCK1* overexpression was relatively modest compared to that observed upon *SIP4* deletion (Fig. 4C). This observation suggests that *PCK1* may not be the principal factor driving production enhancement, implicating the involvement of other factors with substantial influence on metabolic suitability.

In order to find out these factors, all significantly differentially expressed genes with a proper transcriptional level (Ilog2fold changeI ≥1.5, FPKM ≥20.0) in GA184-ΔSIP4 were tested. Considering that the FPKM values of the significantly downregulated genes fell below 5.0, we focused on the significantly upregulated genes by overexpressing them in the GA184 strain to assess their impact on triterpenoid production (Supporting Information Table S4).

Of note, this investigation led to the discovery of *PHO89*, a phosphate (Pi) transporter gene, whose overexpression in GA184 resulted in a licorice triterpenoid production identical to *SIP4*-deleted strain (Fig. 4C). Compared to GA184, the inner Pi content was significantly increased both during the rapid synthesis stage of licorice triterpenoids at 48 h and by the end of fermentation at 120 h when deleting *SIP4* or overexpressing *PHO89* (Fig. 4D). The increased inner Pi would facilitate the carbon source entering into catabolic pathway such as glycolysis rather than the 'storage' carbohydrate[38], which promoted more metabolic flux towards product synthesis. Consequently, we observed a notable reduction in the accumulation of trehalose, a major 'storage' carbohydrate that accumulates in cells[39], in strains with *SIP4* deletion and *PHO89* overexpression at 48 h and 120 h (Fig. 4E). In contrast, there was a significant decrease in licorice triterpenoid production when trehalose synthesis was enhanced through the overexpression of *TPS1* (Fig. S4D and E).

Increased phosphate absorption can also enhance ATP production, leading to higher energy levels within the yeast cells. This can positively impact cellular processes that require energy, such as MVA pathway. Producing 1mol licorice triterpenoids from MVA would consuming 12 mol ATP[40]. Compared to GA184, 0.32 mmol/L more licorice triterpenoids were produced by GA182-ΔSIP4, indicating at least 3.84 mmol/L more ATP was produced. However, due to the dynamic consumption of ATP, the ATP assay displayed no significant difference in these strains (Fig. S4F).

These findings suggested that the manipulation of phosphate absorption can serve as a means to reconfigure yeast metabolism, redirecting metabolic flux away from the accumulation of "storage" carbohydrates in favor of heightened product synthesis, concomitant with an augmentation in ATP generation (Fig. 4F). This concerted effect substantially bolstered yeast's suitability for the biosynthesis of diverse compounds. Notably, such metabolic reprogramming can be readily accomplished through the straightforward deletion of *SIP4*, thereby unveiling an innovative and simple metabolic engineering strategy. Consequently, by merely operating two genes, *NHMGR* and *SIP4*, we successfully established a favorable framework in yeast, resulting in a substantial increase in licorice triterpenoid production.

---

triterpenoids production that involves the upregulation of a set of genes (in green and orange) governing key processes within the glyoxylate cycle, gluconeogenesis, cytoplasmic acetyl-CoA supply, mitochondrial transporters (left); and the scheme for deploying *NHMGR* (right). (F) Overexpression of *NHMGR* sharply increased the licorice triterpenoid production. (G) Overexpression of *NHMGR* sharply increased the precursor β-amyrin production. (H) The NADPH level of GA182 and GA184 at 24 and 48 h. (I) The production of squalene in GA182 and GA184. (J) Overexpression of *NHMGR* did not influence the transcriptional level of MVA pathway. Asterisks indicate statistical significance as determined by paired Student's *t*-test (*$P < 0.05$; **$P < 0.01$). Data are presented as mean ± SD ($n = 3$ biologically independent samples).
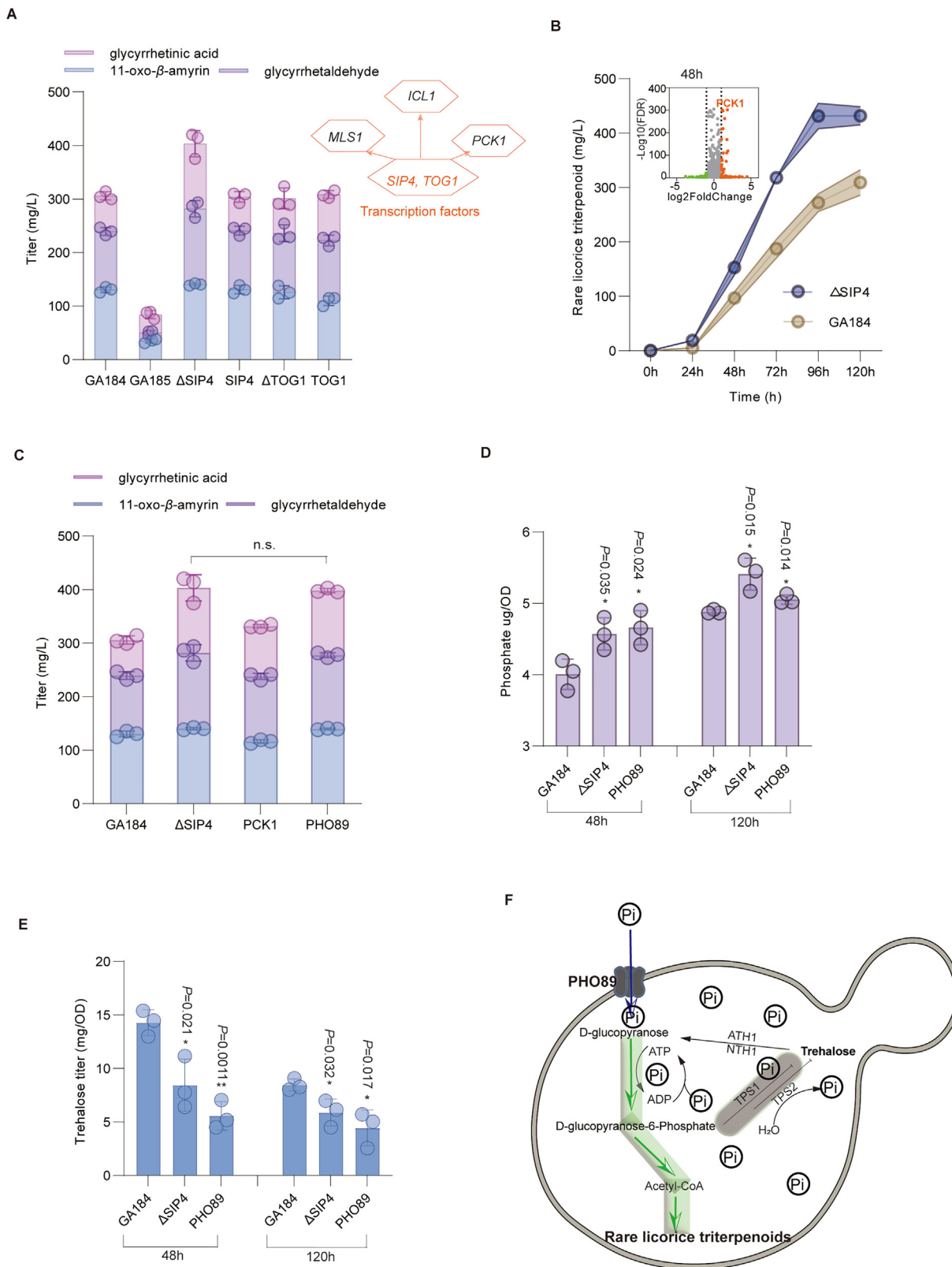
Figure 4 Redesigning yeast metabolism to enhance the suitability. (A) Deleting the transcription factor *SIP4* significantly promoted the licorice triterpenoid production. (B) Fermentation performance of GA184 and GA184-Δ*SIP4* in flask. (C) The upregulated *PHO89* underpins the promotion of licorice triterpenoids. (D) The inner phosphate content of GA184 is significantly lower than that in GA184-Δ*SIP4* at both rapid synthesis stage of licorice triterpenoids and the end of fermentation. (E) Deleting *SIP4* led to significantly decreased trehalose accumulation at both rapid synthesis stage of licorice triterpenoids and the end of fermentation. (F) Promoted phosphate intake by the up-regulated PHO89 would drive more carbon flux to triterpenoid biosynthesis rather than the trehalose; green arrows indicate enhanced pathways. Asterisks indicate statistical significance as determined by paired Student's *t*-test (*$P < 0.05$; **$P < 0.01$), Data are presented as mean $\pm$ SD ($n = 3$ biologically independent samples), n.s. means no significant difference.
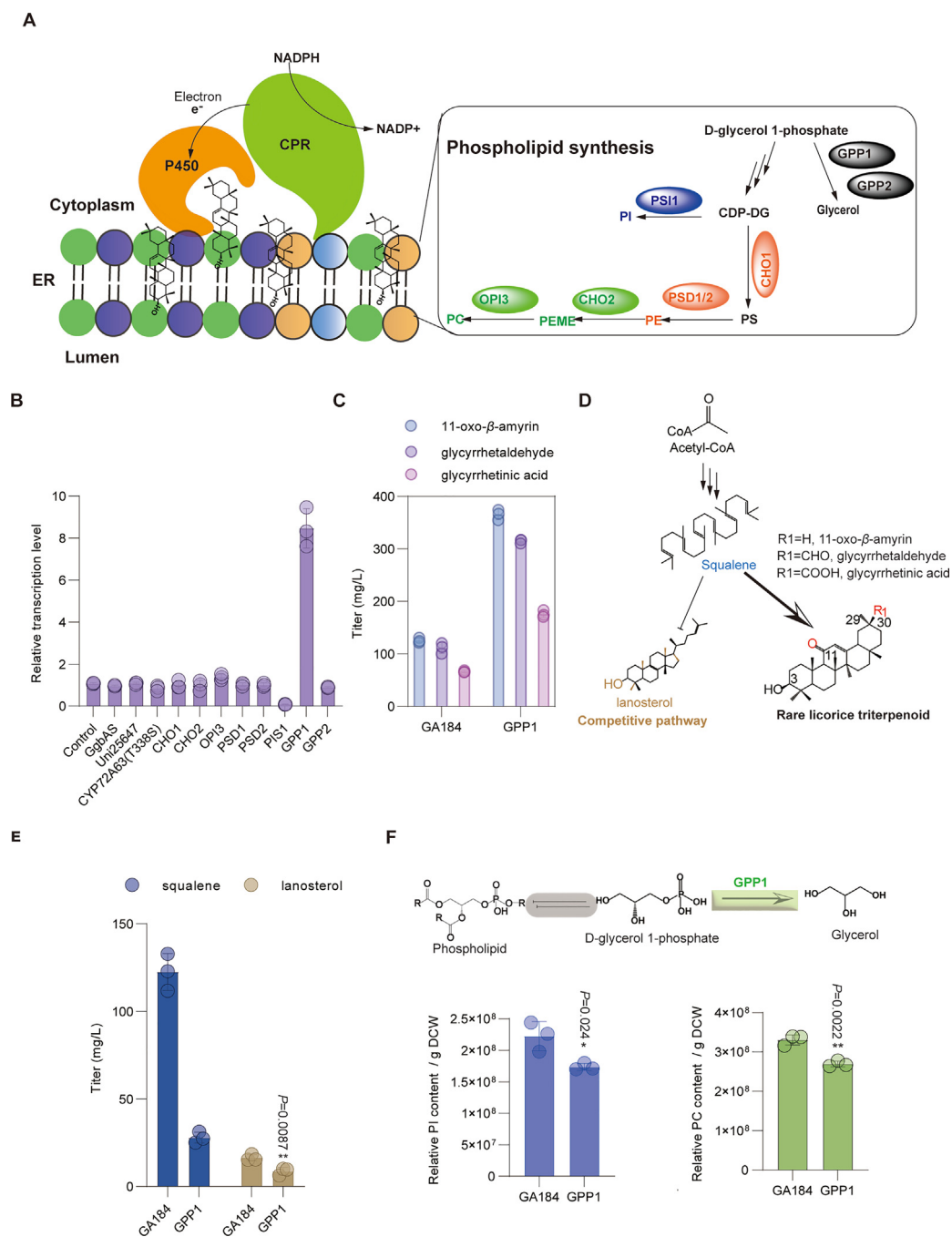
Figure 5 Manipulating phospholipid microenvironment intensified P450 performance in yeast. (A) The overview of ER localized P450s and phospholipid biosynthesis pathway. PSI1: 2-acyl-1-lysophosphatidylinositol acyltransferase, CHO1: Phosphatidylethanolamine *N*-methyltransferase, PSD1/2: Phosphatidylserine decarboxylase proenzyme 1/2, CHO2: Phosphatidylethanolamine *N*-methyltransferase, OPI3: Phosphatidyl-*N*-methylethanolamine *N*-methyltransferase, GPP1/2: Glycerol-1-phosphate phosphohydrolase 1/2. (B) The relative transcription level of key genes related to licorice triterpenoid, phospholipid and glycerol biosynthesis at 48 h compared to that at 24 h in GA184. (C) Overexpression of *GPP1* sharply boosted the P450s' performance. (D) The overview of licorice triterpenoid pathway and its competitive pathway. (E) Overexpression of *GPP1* sharply decreased the accumulation of squalene and compounds from competitive pathway, indicating more metabolic flux was directed to licorice triterpenoid. (F) Overexpression of *GPP1* decreased the PI and PC content of ER. PI, phosphatidylinositol, PC, phosphatidylcholine; Asterisks indicate statistical significance as determined by paired Student's *t*-test (*$P < 0.05$; **$P < 0.01$), Data are presented as mean $\pm$ SD ($n = 3$ biologically independent samples); n.s. means no significant difference.

3.4. Creating microenvironment suitability to further intensify triterpenoid biosynthesis

In addition to the promoted rare licorice triterpenoid biosynthetic pathway, it is noteworthy that GA184 exhibits an augmented production of the competitive product lanosterol (Supporting Information Fig. S5A). This observation highlighted the constraints associated with the ability of heterogenous pathway to divert carbon flux away from the competitive pathway. Apart from the enzymes themselves, the microenvironment surrounding enzymes also plays a significant role in their catalytic activities[22,23]. As endoplasmic reticulum (ER) located membrane proteins, the membrane composition becomes a critical aspect of the microenvironment. As a result, beside the fundamental considerations of NADPH provision and carbon flux regulation, it is imperative to recognize the influence of the ER phospholipid microenvironment on the performance of ER-located plant P450s in yeast (Fig. 5A). Assessing the suitability of yeast phospholipid microenvironment for facilitating the high performance of plant P450s has been a relatively overlooked dimension. In pursuit of identifying potential regulation targets to optimize phospholipid microenvironment, transcriptional analysis was conducted from the reconfigured cellular metabolic profile of GA184 at the 24 and 48 h.

This analysis encompassed pathway genes involved in licorice triterpenoid biosynthesis, namely GgbAS, Uni25647 (F222Y), and CYP72A63 (T338S), as well as key genes associated with phospholipid biosynthesis and turnover, including *PIS1*, *CHO1*, *CHO2*, *OPI3*, *PSD1*, and *PSD2* (Fig. 5A). Notably, only the expression of *PIS1*, encoding the enzyme phosphatidylinositol synthase, exhibited a significant down-regulation, while the expression levels of the remaining genes showed no significant difference between the 24 and 48 h time points (Fig. 5B). The observed decrease in phosphatidylinositol (PI) content (Fig. S5B), concomitant with the down-regulation of *PIS1*, suggests a potential preference for decreased PI content by Uni25647 and CYP72A63 (T338S). Additionally, it is well-established that glycerol plays a crucial role in maintaining P450 stability[41]. The transcriptional analysis of key genes involved in glycerol synthesis, specifically *GPP1* and *GPP2*, revealed a significant up-regulation of *GPP1* expression (Fig. 5B).

Due to the essential nature of *PIS1* gene, the lethality of its deletion, and its tendency to be downregulated to extremely low levels (Fig. 5B), *GPP1* was selected as a target for regulation and subsequent overexpression in the GA184 strain, aiming to further enhance the P450 performance. Notably, this approach resulted in a substantial increase in licorice triterpenoid production, reaching 856.05 ± 16.27 mg/L, accompanied by reduced precursor squalene levels and diminished lanosterol production (Fig. 5C–E). These findings indicated a redirection of metabolic flux towards the desired rare licorice triterpenoids biosynthesis and improved P450s performance. Higher catalytic activity of P450s were observed in microsomes derived from strains overexpressing *GPP1* compared to GA184 (Fig. S5C). Despite the observed elevation in glycerol production resulting from *GPP1* overexpression (Fig. S4D), the addition of glycerol in the culture medium did not exert a significant influence on triterpenoid production (Fig. S5E), suggesting that the enhanced production is not attributable to increased glycerol availability. Considering *sn*-glycerol 3-phosphate as a precursor for phospholipid synthesis, the augmented conversion of *sn*-glycerol 3-phosphate to glycerol may also impact cellular phospholipid content. Lipidomics analysis of the endoplasmic reticulum (ER) revealed a remodeled phospholipid profile characterized by a notable decrease in phosphatidylinositol (PI) and phosphatidylcholine (PC) contents upon *GPP1* overexpression (Fig. 5F, Fig. S5F).

Previous studies have shown that adding phospholipid precursors can promote phospholipid synthesis[42,43]. Hence, the precursor molecules, inositol and choline chloride, were added in the culture medium to promote synthesis of PI (phosphatidylinositol) and PC (phosphatidylcholine) in GA184 and the *GPP1* overexpressing strain, respectively. The results indicated that increasing PI inhibited P450s performance, and increasing PC had no effect (Fig. S5G). Therefore, downregulating PI syntheses was key to create a phospholipid microenvironment favorable for P450s performance for rare licorice triterpenoids synthesis. The decreased content of anionic phospholipids PI up-regulated the membrane charge which may promote the electron transferring from CPR to P450s, leading to promoted P450 performance. These findings indicated that manipulating the membrane microenvironment is an effective strategy for enhancing the efficiency of membrane-bound P450s in yeast. In addition, up-regulating *GPP1* extends the lifespan of yeast, which implies better robustness and genomic stability[44,45], implicating the overexpression of *GPP1* would be favorable for high-level licorice triterpenoid production.

Finally, combining the metabolic and microenvironmental suitability by the deletion of *SIP4* coupled to overexpressing *GPP1* (strain GA188), We achieved an increased titer up to 919.47 ± 15.77 mg/L in flask, and the conversion rate of glucose to licorice triterpenoids further increased from 1.52% to 4.60% (Fig. S5H).

3.5. Fermentation optimization enabled high-level production of rare licorice triterpenoids

The use of YPD-based medium, containing expensive peptone and a previously described synthetic medium by van Hoek et al.[46] including a series of growth factors, is a common practice in fermentation for terpenoids. However, the high cost of peptone and the complexity of the synthetic media made it unsuitable for commercial production. In order to reduce the medium costs and optimize the production of rare licorice triterpenoids, the impact of various nitrogen sources on the production was evaluated by conducting flask experiments. Substituting 10 g/L of corn steep liquor for 20 g/L of peptone significantly increased the production of licorice triterpenoids to 1209.27 ± 7.37 mg/L, while promoting cell growth (Fig. 6A and B). This substitution resulted in a 47.31% reduction in medium cost, providing a more practical commercial production scheme.

To evaluate the performance of GA188, a two-stage fed-batch strategy was employed in 5 L bioreactors using the optimized medium. In the first stage, glucose was added at 12 h after the initial glucose was completely consumed and maintained below 0.1 g/L concentration to avoid repression of the Gal promoters, which controlled the expression of Uni25647(F222Y) and CYP72A63(T338S). The resultant biomass had an OD_{600} level of approximately 140 at 48 h. In the second stage, ethanol was fed at 48 h with a concentration maintained at about 7 g/L, and a constant flow velocity of 5 mL/h was maintained for the nutrient solution containing 10 g/L yeast extraction and 10 g/L corn steep liquor throughout the second stage. Finally, a high-level licorice triterpenoid production of 4.92 g/L was achieved with a productivity of 41.04 mg/L/h, including 0.96 g/L of 11-oxo-β-amyrin,
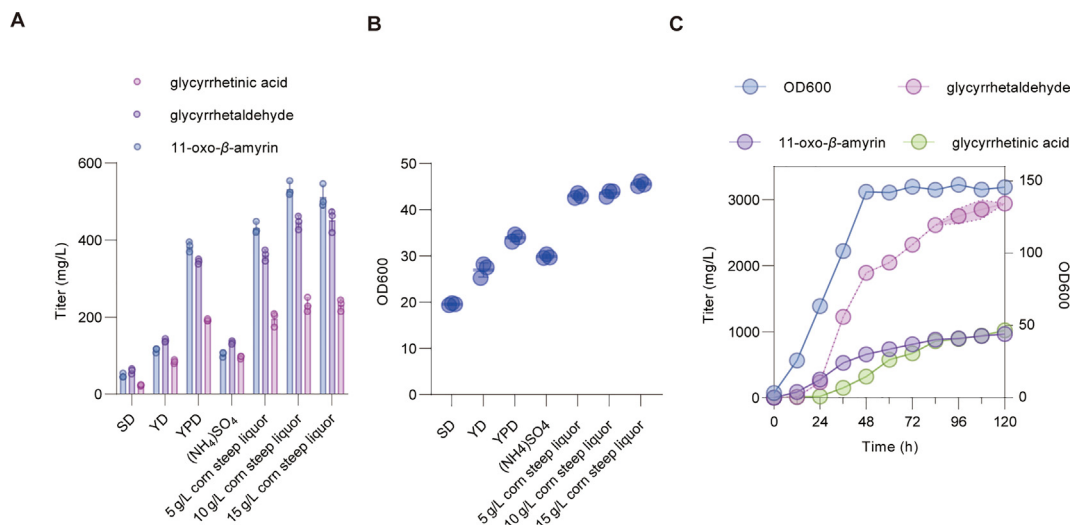
Figure 6 Fermentation optimization enabled high-level production of licorice triterpenoids. (A) Substituting 10 g/L of corn steep liquor for 20 g/L of peptone significantly increased the production of licorice triterpenoids. SD, the cultural medium described previously[46]; Y, Yeast extraction; P, peptone; D, D-glucose; YD, the cultural medium containing 10 g/L yeast extraction, 20 g/L glucose. Ammonium sulfate (5 g/L) and corn steep liquor (10 and 15 g/L) were added in YD as substitutive nitrogen sources. (B) The influence of various nitrogen source on cell growth. Substituting 10 g/L of corn steep liquor for 20 g/L of peptone significantly increased the cell growth. (C) Fed-batch fermentation of GA188 in 5 L fermenter. Data are presented as mean $\pm$ SD ($n = 3$ biologically independent samples).

2.94 g/L of glycyrrhetaldehyde, and 1.02 g/L glycyrrhetinic acid (Fig. 6C), possessing a great potential for commercial application.

4. Discussions

Despite advancements in pharmaceutical chemical production through microbial cell factories, significant challenges persist due to the restricted availability of highly active enzymes and incomprehensive understanding of cell and pathway compatibility, both of which hinder high productivity. P450 enzymes play a pivotal role in the biosynthesis of diverse natural pharmaceutical compounds, encompassing terpenoids, flavonoids, and alkaloids. P450 performance within microbial cell factories is widely acknowledged as the primary limiting factor. Two principal approaches have emerged for augmenting P450 functionality: modulation of the P450: CPR ratio and enzyme engineering. The fine adjustment of the P450: CPR expression ratio stands as a direct method to enhance P450 activity. Implementation of this approach resulted in a notable advance in the production of 11-oxo-β-amyrin, yielding 810.6 mg/L in fed-batch fermentation. Nevertheless, this strategy encounters constraints in achieving further activity enhancement due to inherent limitations stemming from enzyme structural characteristics.

Protein engineering has emerged as a successful strategy to surmount these limitations. Nonetheless, for membrane-bound enzymes such as P450s, the absence of crystal structures and high-throughput detection methods poses a formidable challenge to efficient engineering. In this investigation, we leveraged the recently developed AlphaFold2 to predict the three-dimensional structure of Uni25647 and elucidate its interaction with the substrate β-amyrin. Our analysis unveiled the role of the hydrophobic microenvironment within the substrate tunnel in repelling the hydroxy group of β-amyrin, with F222 identified as a pivotal determinant of tunnel characteristics. These insights led to the

discovery of mutant F222Y, which exhibited substantially enhanced activity and was derived from a compact mutagenesis library focusing solely on saturation mutagenesis at the F222 site. This modification led to a remarkable elevation in 11-oxo-β-amyrin production, reaching 1598.53 mg/L, doubling the output of prior research endeavors. Our findings advocate for an efficacious strategy to amplify the microbial synthesis of natural pharmaceutical compounds by optimizing the performance of key P450s through aligning the substrate tunnel microenvironment with substrate properties.

Besides the inherent characteristics of enzymes, their catalytic efficacy is extensively influenced by the surrounding microenvironment. Therefore, manipulating the microenvironment around the enzymes presents a tertiary avenue to fortify their performance. Particularly, membrane-bound enzymes are susceptible to modulation of the phospholipid microenvironment, thereby exerting a pronounced influence on their activity. However, engineering endeavors often overlook the crucial aspect of regulating membrane phospholipids to render the host cell microenvironment more conducive for heterologous enzymes, notably the rate-limiting P450s. The intricate regulatory mechanisms governing the synthesis and turnover of glycerophospholipids and glycerolipids pose significant challenges in pinpointing suitable regulatory targets directly from their biosynthetic pathways, which is crucial for constructing a specific phospholipid model conducive to achieving desired outcomes *in vivo*[47,48]. Despite these challenges, our investigation elucidated that overexpression of *GPP1* induces alterations in phospholipid composition, culminating in the establishment of a microenvironment characterized by reduced PI content within the ER membrane. This engineered milieu further enhanced the performance of engineered P450s, resulting in a marked increase in licorice triterpenoid production. This discovery holds considerable significance as it unveils the potential for manipulating the membrane microenvironment to enhance P450 performance in yeast. Additionally, these findings offer insights into potential targets for

modulating lipid biosynthesis. In the future, genome-scale metabolic engineering strategies targeting all relevant genes could represent a viable approach to identify engineering targets aimed at establishing phospholipid homeostasis conducive to key enzymes in plant natural product biosynthesis. Notably, enhancing the host internal microenvironment suitability for heterologous enzymes can serve as an efficient strategy to amplify their performance in producing natural pharmaceutical compounds.

In the realm of pathway optimization, the limited comprehension of metabolic suitability for plant triterpenoid biosynthesis has rendered many conventional strategies somewhat uninformed and complicated, often necessitating extensive gene editing[49]. For instance, prior metabolic engineering endeavors aimed at augmenting the metabolic flux towards triterpenoids primarily concentrated on enhancing acetyl-CoA derived from glucose metabolism[50]. However, glucose undergoes rapid conversion to ethanol during the initial phases of fermentation, thereby establishing ethanol as the principal carbon source (Fig. 3B) when yeast exhibits superior suitability for plant triterpenoid biosynthesis. Through meticulous tracking of metabolic rearrangements, we delineated the metabolic framework underpinning this suitability, which revolves around gluconeogenesis and the glyoxylate cycle, accompanied by augmented cofactor and acetyl-CoA provisioning. Building upon this understanding, we devised an exceedingly straightforward strategy to establish a conducive metabolic framework for intensified plant triterpenoid biosynthesis, concurrently enhancing precursor supply, cofactor availability, and P450 performance, by overexpressing a single gene, the NADH-dependent HMG-CoA reductase (*NHMGR*) from *Silicibacter pomeroyi*[51,52]. Fostering metabolic compatibility between the biosynthetic pathway and the host cell holds immense promise for constructing microbial cell factories efficiently and succinctly, thereby facilitating the proficient synthesis of natural product drugs. Additionally, given the notable efficiency of the direct pathway refinement strategy, exemplified by its success in bolstering the MVA pathway to produce triterpenoid precursors like squalene, which achieved a titer of 9472 mg/L[32], there is also potential for enhancing natural product production by optimizing the synergy between the host organism that produces precursors and the target pathways.

Furthermore, within the fermentation process, trehalose accumulates in response to alterations in culture conditions. However, its accumulation entails a diversion of carbon flux away from triterpenoid biosynthesis and disrupts the reactivation of denatured proteins facilitated by heat shock proteins[53]. Herein, these challenges were effectively addressed, and the metabolic landscape conducive to efficient triterpenoid biosynthesis was further enhanced through the deletion of the transcriptional factor *SIP4*. The removal of *SIP4* facilitated a redirection of carbon flux towards licorice triterpenoids rather than trehalose accumulation, achieved by augmenting phosphate uptake *via* the upregulation of *PHO89*, which encodes a phosphate transporter. Our findings propose a novel paradigm for enhancing the production of target compounds: orchestrating the redirection of carbon flux from storage sugars such as trehalose to target compounds through the optimization of phosphate homeostasis.

5. Conclusions

In summary, a Uni25647 mutant with higher activity was created by enzyme engineering. By manipulating only 3 genes, *NHMGR*, *GPP1* and *SIP4*, the yeast's cell suitability was established for plant triterpenoid biosynthesis with simultaneously enhanced carbon flux, cofactor availability and performance of ER-localized, rate-limiting plant P450s. Combined with fermentation optimization, the production of rare licorice triterpenoid reached up to 4.92 g/L with a productivity of 41.04 mg/L/h, including 0.96 g/L of 11-oxo-β-amyrin, 2.94 g/L of glycyrrhetaldehyde and 1.02 g/L of glycyrrhetinic acid, and the fermentation medium cost was significantly decreased by 47.31% *via* substituting the expensive peptone with corn steep liquor. These results demonstrate the commercial potential and provide new perspectives for efficient heterologous biosynthesis of plant natural products in yeast.

Author contributions

Wentao Sun: Writing − review & editing, Writing − original draft, Methodology, Investigation, Formal analysis. Shengtong Wan: Validation, Investigation. Chuyan Liu: Writing − original draft, Formal analysis, Data curation. Ruwen Wang: Writing − review & editing, Software, Formal analysis. Haocheng Zhang: Investigation, Formal analysis, Data curation. Lei Qin: Writing − review & editing, Software, Resources, Methodology. Runming Wang: Writing − review & editing, Data curation. Bo Lv: Writing − review & editing, Writing − original draft, Project administration, Methodology, Investigation, Formal analysis. Chun Li: Writing − review & editing, Supervision, Resources, Project administration, Methodology, Investigation, Data curation.

Conflicts of interest

The authors declare no conflicts of interest.

Appendix A.   Supporting information

Supporting information to this article can be found online at https://doi.org/10.1016/j.apsb.2024.04.032.

References

1. Yu VY, Chang MC. High-yield chemical synthesis by reprogramming central metabolism. *Nat Biotechnol* 2016;**34**:1128−9.
2. Li S, Li Y, Smolke CD. Strategies for microbial synthesis of high-value phytochemicals. *Nat Chem* 2018;**10**:395−404.
3. Dinday S, Ghosh S. Recent advances in triterpenoid pathway elucidation and engineering. *Biotechnol Adv* 2023;**68**:108214.
4. Zhang R, Li C, Wang J, Yang Y, Yan Y. Microbial production of small medicinal molecules and biologics: from nature to synthetic pathways. *Biotechnol Adv* 2018;**36**:2219−31.
5. Jiang F, Zhou C, Li Y, Deng H, Gong T, Chen J, et al. Metabolic engineering of yeasts for green and sustainable production of bioactive ginsenosides F2 and 3β,20S-Di-O-Glc-DM. *Acta Pharm Sin B* 2022;**12**:3167−76.

6. Duan Y, Du W, Song Z, Chen R, Xie K, Liu J, et al. Functional characterization of a cycloartenol synthase and four glycosyl-transferases in the biosynthesis of cycloastragenol-type astragalosides from *Astragalus membranaceus*. *Acta Pharm Sin B* 2023;**13**:271−83.

7. Chen R, Gao J, Yu W, Chen X, Zhai X, Chen Y, et al. Engineering cofactor supply and recycling to drive phenolic acid biosynthesis in yeast. *Nat Chem Biol* 2022;**18**:520−9.

8. Zhu M, Wang C, Sun W, Zhou A, Wang Y, Zhang G, et al. Boosting 11-oxo-beta-amyrin and glycyrrhetinic acid synthesis in *Saccharomyces cerevisiae via* pairing novel oxidation and reduction system from legume plants. *Metab Eng* 2018;**45**:43−50.

9. Pompei R, Flore O, Marccialis MA, Pani A, Loddo B. Glycyrrhizic acid inhibits virus growth and inactivates virus particles. *Nature* 1979;**281**:689.

10. Shimoyama Y, Hirabayashi K, Matsumoto H, Sato T, Shibata S, Inoue H. Effects of glycyrrhetinic acid derivatives on hepatic and renal 11β-hydroxysteroid dehydrogenase activities in rats. *J Pharm Pharmacol* 2003;**55**:811−7.

11. Xiao Y, Xu J, Mao C, Jin M, Wu Q, Zou J, et al. 18Beta-glycyrrhetinic acid ameliorates acute *Propionibacterium acnes*-induced liver injury through inhibition of macrophage inflammatory protein-1alpha. *J Biol Chem* 2010;**285**:1128−37.

12. Sun M, Xin Q, Hou K, Qiu J, Wang L, Chao E, et al. Production of 11-oxo-beta-amyrin in *Saccharomyces cerevisiae* at high efficiency by fine-tuning the expression ratio of CYP450:CPR. *J Agric Food Chem* 2023;**71**:3766−76.

13. Schmid C, Mittermeier-Klessinger V, Tabea Peters VC, Berger F, Kramler M, Heuberger H, et al. Quantitative mapping of flavor and pharmacologically active compounds in european licorice roots (*Glycyrrhiza glabra* L.) in response to growth conditions and arbuscular mycorrhiza symbiosis. *J Agric Food Chem* 2021;**69**:13173−89.

14. Rozen S, Shahak I, Bergmann E. Synthesis and reactions of 18β-glycyrrhetaldehyde. *Tetrahedron* 1973;**29**:2327−31.

15. Wang L, Yang R, Yuan B, Liu Y, Liu C. The antiviral and antimicrobial activities of licorice, a widely-used Chinese herb. *Acta Pharm Sin B* 2015;**5**:310−5.

16. Seki H, Sawai S, Ohyama K, Mizutani M, Ohnishi T, Sudo H, et al. Triterpene functional genomics in licorice for identification of CYP72A154 involved in the biosynthesis of glycyrrhizin. *Plant Cell* 2011;**23**:4112−23.

17. Jin K, Shi X, Liu J, Yu W, Liu Y, Li J, et al. Combinatorial metabolic engineering enables the efficient production of ursolic acid and oleanolic acid in *Saccharomyces cerevisiae*. *Bioresour Technol* 2023;**374**:128819.

18. Ma T, Shi B, Ye Z, Li X, Liu M, Chen Y, et al. Lipid engineering combined with systematic metabolic engineering of *Saccharomyces cerevisiae* for high-yield production of lycopene. *Metab Eng* 2019;**52**:134−42.

19. Wong J, de Rond T, d'Espaux L, van der Horst C, Dev I, Rios-Solis L, et al. High-titer production of lathyrane diterpenoids from sugar by engineered *Saccharomyces cerevisiae*. *Metab Eng* 2018;**45**:142−8.

20. Gao J, Zuo Y, Xiao F, Wang Y, Li D, Xu J, et al. Biosynthesis of catharanthine in engineered *Pichia pastoris*. *Nat Synth* 2023;**2**:231−42.

21. Sun W, Xue H, Liu H, Lv B, Yu Y, Wang Y, et al. Controlling chemo- and regioselectivity of a plant p450 in yeast cell toward rare licorice triterpenoid biosynthesis. *ACS Catal* 2020;**10**:4253−60.

22. Lancaster L, Abdallah W, Banta S, Wheeldon I. Engineering enzyme microenvironments for enhanced biocatalysis. *Chem Soc Rev* 2018;**47**:5177−86.

23. Li YM, Yuan J, Ren H, Ji CY, Tao Y, Wu Y, et al. Fine-tuning the micro-environment to optimize the catalytic activity of enzymes immobilized in multivariate metal-organic frameworks. *J Am Chem Soc* 2021;**143**:15378−90.

24. Xie ZX, Li BZ, Mitchell LA, Wu Y, Qi X, Jin Z, et al. "Perfect" designer chromosome V and behavior of a ring derivative. *Science* 2017;**355**:eaaf4704.

25. Gietz RD, Schiestl RH. High-efficiency yeast transformation using the LiAc/SS carrier DNA/PEG method. *Nat Protoc* 2007;**2**:31.

26. Shao Z, Zhao H, Zhao H. DNA assembler, an *in vivo* genetic method for rapid construction of biochemical pathways. *Nucleic Acids Res* 2008;**37**:e16.

27. Pompon D, Louerat B, Bronine A, Urban P. Yeast expression of animal and plant P450s in optimized redox environments. *Methods Enzymol* 1996;**272**:51−64.

28. Gao J, Li Y, Yu W, Zhou YJ. Rescuing yeast from cell death enables overproduction of fatty acids from sole methanol. *Nat Metab* 2022;**4**:932−43.

29. Wang X, Liu W, Xin C, Zheng Y, Cheng Y, Sun S, et al. Enhanced limonene production in cyanobacteria reveals photosynthesis limitations. *Proc Natl Acad Sci U S A* 2016;**113**:14225−30.

30. Baek M, DiMaio F, Anishchenko I, Dauparas J, Ovchinnikov S, Lee GR, et al. Accurate prediction of protein structures and interactions using a three-track neural network. *Science* 2021;**373**:871−6.

31. Meadows AL, Hawkins KM, Tsegaye Y, Antipov E, Kim Y, Raetz L, et al. Rewriting yeast central carbon metabolism for industrial isoprenoid production. *Nature* 2016;**537**:694−7.

32. Li T, Liu GS, Zhou W, Jiang M, Ren YH, Tao XY, et al. Metabolic engineering of *Saccharomyces cerevisiae* to overproduce squalene. *J Agric Food Chem* 2020;**68**:2132−8.

33. Yukawa T, Bamba T, Guirimand G, Matsuda M, Hasunuma T, Kondo A. Optimization of 1,2,4-butanetriol production from xylose in *Saccharomyces cerevisiae* by metabolic engineering of NADH/NADPH balance. *Biotechnol Bioeng* 2021;**118**:175−85.

34. Cherry JM, Hong EL, Amundsen C, Balakrishnan R, Binkley G, Chan ET, et al. Saccharomyces genome database: the genomics resource of budding yeast. *Nucleic Acids Res* 2011;**40**:D700−5.

35. Thepnok P, Ratanakhanokchai K, Soontorngun N. The novel zinc cluster regulator Tog1 plays important roles in oleate utilization and oxidative stress response in *Saccharomyces cerevisiae*. *Biochem Biophys Res Commun* 2014;**450**:1276−82.

36. Lesage P, Yang X, Carlson M. Yeast SNF1 protein kinase interacts with SIP4, a C6 zinc cluster transcriptional activator: a new role for SNF1 in the glucose response. *Mol Cell Biol* 1996;**16**:1921−8.

37. Han BK, Emr SD. The phosphatidylinositol 3,5-bisphosphate (PI(3,5) P2)-dependent Tup1 conversion (PIPTC) regulates metabolic reprogramming from glycolysis to gluconeogenesis. *J Biol Chem* 2013;**288**:20633−45.

38. van Heerden JH, Wortel MT, Bruggeman FJ, Heijnen JJ, Bollen YJ, Planque R, et al. Lost in transition: start-up of glycolysis yields subpopulations of nongrowing cells. *Science* 2014;**343**:1245114.

39. Gupta R, Laxman S. Cycles, sources, and sinks: conceptualizing how phosphate balance modulates carbon flux using yeast metabolic networks. *Elife* 2021;**10**:e63341.

40. Pauwels GB. A study of the factors causing a decrease in the rate of phosphate uptake by yeast during phosphate accumulation. *Acta Bot Neerl* 1967;**16**:125−31.

41. Guengerich FP, Martin MV, Sohl CD, Cheng Q. Measurement of cytochrome P450 and NADPH-cytochrome P450 reductase. *Nat Protoc* 2009;**4**:1245−51.

42. Hallman M, Epstein BL. Role of myo-inositol in the synthesis of phosphatidylglycerol and phosphatidylinositol in the lung. *Biochem Bioph Res Co* 1980;**92**:1151−9.

43. Gasull T, DeGregorio-Rocasolano N, Zapata A, Trullas R. Choline release and inhibition of phosphatidylcholine synthesis precede excitotoxic neuronal death but not neurotoxicity induced by serum deprivation. *J Biol Chem* 2000;**275**:18350−7.

44. Correia-Melo C, Kamrad S, Tengolics R, Messner CB, Trebulle P, Townsend S, et al. Cell−cell metabolite exchange creates a pro-survival metabolic environment that extends lifespan. *Cell* 2023;**186**:63−79.e21.

45. Bitterman KJ, Medvedik O, Sinclair DA. Longevity regulation in *Saccharomyces cerevisiae*: linking metabolism, genome stability, and heterochromatin. *Microbiol Mol Biol Rev* 2003;**67**:376−99.

46. van Hoek P, van Dijken JP, Pronk JT. Regulation of fermentative capacity and levels of glycolytic enzymes in chemostat cultures of

Saccharomyces cerevisiae. *Enzym Microb Technol* 2000;**26**: 724−36.

47. Henry SA, Kohlwein SD, Carman GM. Metabolism and regulation of glycerolipids in the yeast *Saccharomyces cerevisiae*. *Genetics* 2012; **190**:317−49.

48. Jin Z, Vighi A, Dong Y, Bureau JA, Ignea C. Engineering membrane architecture for biotechnological applications. *Biotechnol Adv* 2023; **64**:108118.

49. Campbell K, Xia J, Nielsen J. The impact of systems biology on bioprocessing. *Trends Biotechnol* 2017;**35**:1156−68.

50. Cardenas J, Da Silva NA. Engineering cofactor and transport mechanisms in *Saccharomyces cerevisiae* for enhanced acetyl-CoA and polyketide biosynthesis. *Metab Eng* 2016;**36**:80−9.

51. Paddon CJ, Westfall PJ, Pitera DJ, Benjamin K, Fisher K, McPhee D, et al. High-level semi-synthetic production of the potent antimalarial artemisinin. *Nature* 2013;**496**:528−32.

52. Sun W, Qin L, Xue H, Yu Y, Ma Y, Wang Y, et al. Novel trends for producing plant triterpenoids in yeast. *Crit Rev Biotechnol* 2019;**39**:618−32.

53. Eleutherio E, Panek A, De Mesquita JF, Trevisol E, Magalhaes R. Revisiting yeast trehalose metabolism. *Curr Genet* 2015;**61**:263−74.